Energy Proceedings
Vol 60, 2025
ISSN 2004-2965

Fault Location Algorithm for Distribution Networks Based on Differential Current Matrix

Pinghao Ni[1], Yuancun Nie[1], Meng Li[1], Jinghan He[1], Wenjia Ma[1]

1 School of Electrical Engineering, Beijing Jiaotong University

Haidian District, Beijing 100044, P.R.China

ABSTRACT

To address the challenges in distribution network protection caused by high-penetration distributed generation (DG) integration, this study proposes a multi-source information fusion-based fault location algorithm for distribution networks. A dynamic current matrix for fault zones and a topology-adaptive node differential matrix are constructed, and the fault location matrix is derived through matrix multiplication. Grounded in the current differential principle for distribution network fault localization, logical analysis is performed on the fault discrimination matrix. PSCAD simulation demonstrated that the criterion is capable of accurately locating fault nodes. The algorithm exhibits advantages such as simplicity in principle, low memory consumption, high computational efficiency, and superior accuracy, demonstrating strong practicality. It provides a robust solution for active distribution networks with high-penetration renewable energy.

Keywords: distribution network, distributed generation, matrix algorithm, fault location

1. INTRODUCTION

As highlighted in Reference [1], research on precise short-circuit fault location technology for distribution networks—a critical power system component—carries significant theoretical and practical importance in enhancing grid security and stability. With the ongoing development of new power systems, active distribution networks have evolved from traditional single-supply operation to complex scenarios incorporating distributed photovoltaics, energy storage, and flexible loads [2]. This transition has severely challenged the adaptability of conventional fault location methods, leading to a marked decline in positioning accuracy [3].

Traditional distribution network fault location methods—such as the matrix algorithm [4], signal injection method [5], traveling wave method [6], and impedance method [7]—exhibit significant limitations: the matrix approach depends on dual-node data integrity and fails during power supply or user-side faults [8]; signal injection is prone to interference from line parasitic parameters [9]; the traveling wave method suffers from low fault-point reflection coefficients, reducing accuracy [10]; and the impedance method is vulnerable to dynamic topology changes and voltage oscillations, causing impedance drift and reliability loss [11].

The integration of high-penetration distributed generation (DG) drives distribution networks toward multi-source heterogeneous topologies, markedly increasing operational complexity [12], thereby necessitating the development of novel fault location technologies with robust topological generalization and dynamic response capabilities [13].

This paper proposes a current differential fault location algorithm for distribution networks. By real-time synchronous acquisition of node current data, a multi-dimensional fault feature matrix is constructed. Based on the theoretical framework of current differential protection, the algorithm outputs fault coordinate parameters corresponding to the physical topology, enabling accurate identification and localization of fault sections under complex operating conditions. The method effectively addresses the anti-interference challenges of traditional approaches in dynamic network reconfiguration scenarios while maintaining low computational complexity.

2. MATRIX-STRUCTURED DATA CONSTRUCTION

Open-loop topology represents one of the most classical and widely adopted network architectures in distribution systems. Its defining characteristic is the absence of closed loops during normal operational conditions. Distribution networks typically employ a closed-loop design with open-loop operation, maintaining a radial topological structure under normal

---

This is a paper for the 5th Applied Energy Symposium and Forum: Renewable Energy Matrix (REM2025), Oct. 29-31, 2025, Yancheng, China.

circumstances. The network configuration can be abstracted using graph theory principles: power sources, loads, and control devices constitute the node set, while connecting lines form the edge set [14]. Through the acquisition of topological parameters and electrical measurement data, mathematical representations such as correlation matrices and admittance matrices are constructed, enabling the application of matrix-based analytical methods for fault location purposes.

As illustrated in Figure 1, a systematic matrix analysis-based fault location system can be constructed for distribution networks under open-loop operation topology. First, leveraging the Wide Area Measurement System (WAMS), current amplitude and phase information from each feeder branch are collected in real-time [15]. Following data standardization, a dynamic current matrix with spatiotemporal correlation characteristics is formed. The dimensions of this matrix correspond to the product of the number of network branches and the sampling time window.

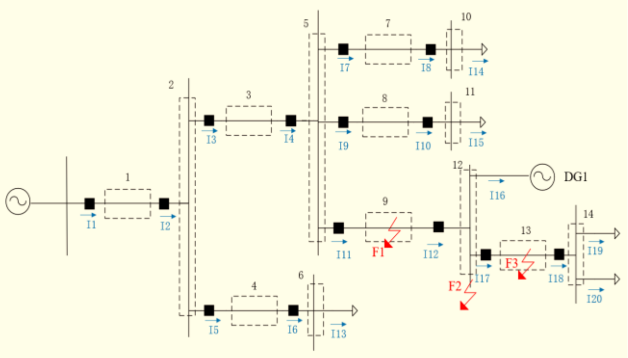

Fig. 1 Open-loop structure of distribution network

Subsequently, based on topological modeling theory, the dotted sections in the graph—specifically, the connection points between feeder segments linked to switching devices and the bus—are abstracted as matrix nodes and numbered sequentially as node *i* (*i*= 0, 1, ..., 14). The switch-node correlation is characterized using an adjacency matrix, while a binary nodal differential matrix is constructed by incorporating network connectivity characteristics. Matrix elements take values from the set {1, 0, −1} to precisely characterize current relationships at each node: A value of 1 is assigned to nodes where current flows inward relative to the reference direction; A value of −1 is assigned to nodes where current flows outward; A value of 0 is assigned to nodes with no direct correlation.

A fault feature matrix is then generated through matrix multiplication, where non-zero elements correspond to spatial distribution characteristics of potential fault nodes.

Decision rules are established based on the principle of current differential protection. This matrix analysis method enables rapid identification and accurate localization of fault sections in complex distribution networks through multi-source data fusion and feature space mapping.

3. FUNDAMENTAL PRINCIPLES OF THE ALGORITHM

3.1 Fault information current matrix I

Following the matrix construction principles outlined in the previous section, partitions containing exclusively fault information are selected for current data acquisition.

After numbering the network nodes, the direction of the main power supply is designated as the reference, and the direction from the system power source to each branch is defined as the positive direction. Leveraging the Wide Area Measurement System (WAMS), three-phase current amplitude, phase, and transient waveforms from key nodes are collected in real-time via Synchronized Phasor Measurement Units (PMUs) and intelligent terminals (FTUs/DTUs).

This data is used to construct a dynamic current matrix encompassing all loop currents. The resulting current matrix I is expressed as follows:

$$\dot{I} = \begin{bmatrix} \dot{I}_1 \\ \dot{I}_2 \\ \cdots \\ \dot{I}_n \end{bmatrix}$$

In the matrix, n represents the number of distribution network loops. A current matrix encompassing multiple loops is constructed based on the collected fault current information.

3.2 Nodal differential matrix C

The distribution network topology is abstracted as a nodal network interconnected via distribution switches (e.g., circuit breakers, sectional switches). During faults, electrical quantities are synchronously measured across nodes, and a nodal differential matrix C is generated to accurately locate the faulty section.

$$C = \begin{bmatrix} C_{11} & C_{12} & \cdots & C_{1n} \\ C_{21} & C_{22} & \cdots & C_{2n} \\ \cdots & \cdots & \cdots & \cdots \\ C_{m1} & C_{m2} & \cdots & C_{mn} \end{bmatrix}$$

In the above formula, m denotes the number of network nodes within the fault section. For each node i (i= 1, 2, ..., m), the element C_{ij}(j= 1, 2, ..., n) of the differential matrix C characterizes the relationship between the direction of the j-th loop current and node i. The values are assigned as follows: positive direction inflow is recorded as 1, outflow is recorded as −1, and if there is no fault current, it is recorded as 0.

Thus, the directional signals from all nodes collectively form the nodal differential matrix C. The number of columns *n* in C corresponds to the dimension of the loop current vector I, ensuring dimensional consistency for subsequent matrix operations.

3.3 Fault Location Matrix P and Criterion

Upon the occurrence of a fault, the fault location matrix P can be derived through the multiplication of the current matrix I and the nodal differential matrix C:

$$P = CI = \begin{bmatrix} C_{11} & C_{12} & \cdots & C_{1n} \\ C_{21} & C_{22} & \cdots & C_{2n} \\ \cdots & \cdots & \cdots & \cdots \\ C_{m1} & C_{m2} & \cdots & C_{mn} \end{bmatrix} \begin{bmatrix} \dot{I}_1 \\ \dot{I}_2 \\ \cdots \\ \dot{I}_n \end{bmatrix} = \begin{bmatrix} \sum \dot{I}_{\varphi 1} \\ \sum \dot{I}_{\varphi 2} \\ \cdots\cdots \\ \sum \dot{I}_{\varphi m} \end{bmatrix} = \begin{bmatrix} P_{\varphi 1} \\ P_{\varphi 2} \\ \cdots \\ P_{\varphi m} \end{bmatrix}$$

After generating the fault location matrix P based on the current differential principle, the fault location is realized by combining the following judgment basis.

It is stipulated that the current flowing into the node is the positive direction. Under the steady-state condition of the system without fault, it can be judged according to the network topology: if the node is connected with multiple electrical circuits, the branch current satisfies the Kirchhoff current law, and its algebraic sum is zero; if the node is the end node connecting only a single load, its current value is always equal to the load current.

Based on the above principle, the current balance equation of the multi-loop connection node can be derived:

$$P_{\varphi \mathrm{j}} = 0 \quad (\,\mathrm{j}=1,2,\cdots,\mathrm{m}\,) \tag{1}$$

And the current condition formula when the node is connected to a single loop:

$$P_{\varphi \mathrm{j}} = I_{\mathrm{fh}} \tag{2}$$

Where I_{fh} is the load current, based on the formula (1) and formula (2), the action criterion of the node fault in the ideal case is obtained:

$$P_{\varphi \mathrm{j}} \geq I_{\mathrm{set}} \tag{3}$$

In the above formula, $P_{\varphi j}$ is the effective value of each phase current of the node (φ= A phase, B phase, C phase, j= 1, 2... m), and I_{set} is the set current value. When a short-circuit fault occurs outside the zone, the differential protection device should meet the requirements of reliable and non-misoperation when it flows through the maximum possible steady-state or transient unbalanced current:

$$I_{set} = K_k K_{LH} K_f I_{d.\max} \tag{4}$$

In the formula, K_k is the reliability coefficient, K_{LH} is the current transformer ratio error, K_f is the non-periodic component coefficient, $I_{d.max}$is the maximum short-circuit current flowing through the protection device during an external short-circuit event in the bus differential protection zone.

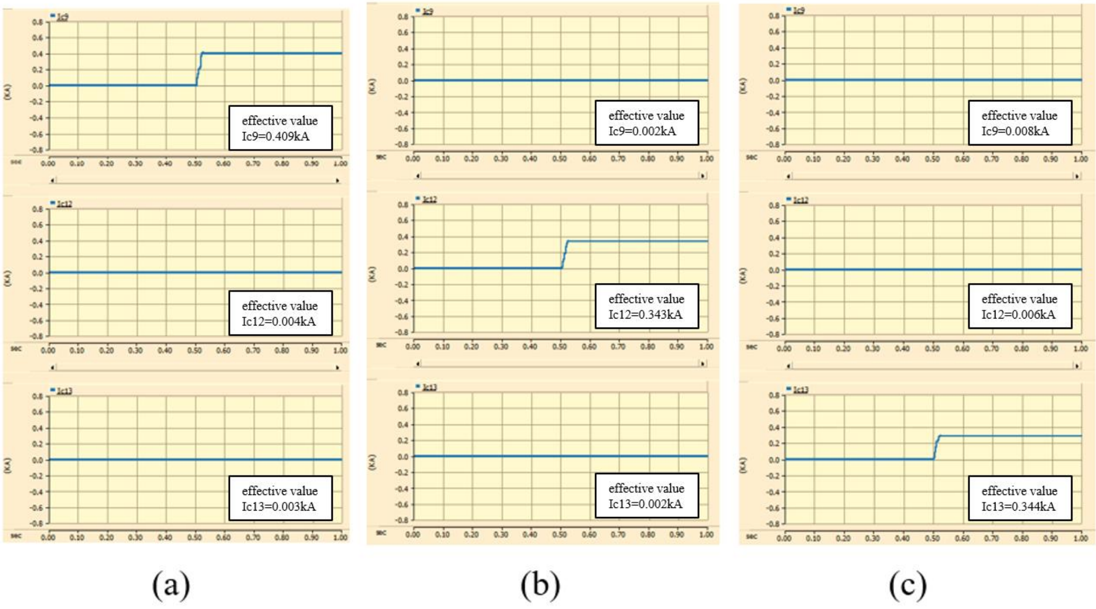

Fig. 2 The effective value waveform of differential current at each node of F1, F2 and F3 faults

When a fault occurs, the specific steps of fault diagnosis by extracting a node element in the fault location matrix P are as follows:

1) Extract a node element $P_{\varphi j}$ (j = 1, 2... m) in the fault location matrix P, and judge whether the node element $P_{\varphi j}$ satisfies the formula (3). If satisfied, it is judged that the fault location is located at the node j.

2) If the node element $P_{\varphi j}$ does not satisfy the formula (3), the j+1 node element in the fault location matrix P is extracted, and the sub-step process is repeated until the fault location is obtained.

4. EXAMPLE ANALYSIS

4.1 Fault-free operation of the system

A 10 kV distribution network model incorporating distributed generation (DG) was implemented in PSCAD, as illustrated in Fig. 1. The network consists of a 5 km line segment and integrates a distributed power source with a capacity of 1 MVA. Fault scenarios F1 to F3 are set at different locations to simulate varying fault conditions.

Following the methodology described earlier, the network nodes were systematically numbered, and 14 equivalent nodes (i.e., m = 14) were defined within the fault zone. The number of current measurement channels was set to n = 20. Given the relatively large number of system nodes, the analysis was simplified by considering only the current matrix elements that exhibit coupling relationships specifically, those corresponding to non-zero entries associated with nodes 9 to 13. The relevant subset of the current matrix is provided below for clarity.

When the distribution line operates under fault-free conditions, the nodal differential matrix C can be constructed according to the methodology detailed in the previous section, as expressed below:

$$C=\begin{bmatrix} \ddots &&&&&&&&&& \\ & C_{9(11)} & C_{9(12)} & \cdots & \cdots & \cdots & \cdots & \cdots & \cdots & 0 & \\ & \vdots & \vdots & \cdots & \cdots & \cdots & \cdots & \cdots & \cdots & \vdots & \\ & \vdots & C_{12(12)} & \cdots & \cdots & \cdots & \cdots & C_{12(16)} & C_{12(17)} & \vdots & \\ & 0 & 0 & \cdots & \cdots & \cdots & \cdots & \cdots & C_{13(17)} & C_{13(18)} & \\ &&&&&&&&&& \ddots \end{bmatrix}$$

$$=\begin{bmatrix} \ddots &&&&&&&&&& \\ & 1 & -1 & \cdots & \cdots & \cdots & \cdots & \cdots & \cdots & 0 & \\ & \vdots & \cdots & \cdots & \cdots & \cdots & \cdots & \cdots & \cdots & \vdots & \\ & \vdots & 1 & 0 & \cdots & \cdots & 0 & 1 & -1 & \vdots & \\ & 0 & \cdots & \cdots & \cdots & \cdots & \cdots & \cdots & 1 & -1 & \\ &&&&&&&&&& \ddots \end{bmatrix}$$

Taking bus node 12 as an example, the expression for the single-loop current is derived using matrix C in conjunction with Equations (1) and (2), as shown below:

$$\begin{aligned} P_{\varphi 12} &= \sum \dot{I}_{\varphi 12} \\ &= C_{12(1)}\dot{I}_1 + C_{12(2)}\dot{I}_2 + \cdots + C_{12(20)}\dot{I}_{20} \\ &= C_{12(12)}\dot{I}_{12} + C_{12(16)}\dot{I}_{16} + C_{12(17)}\dot{I}_{17} \\ &= \dot{I}_{12} - \dot{I}_{16} - \dot{I}_{17} \end{aligned} \tag{5}$$

Similarly, the values of $P_{\varphi j}$ for the remaining line nodes and bus nodes can be derived using the same methodology. By integrating simulated measurement data of currents, the fault location matrix P of the system under fault-free operating conditions can be obtained as follows:

$$P=CI=\begin{bmatrix} \ddots &&&&&&&&&& \\ & 1 & -1 & \cdots & \cdots & \cdots & \cdots & \cdots & \cdots & 0 & \\ & \vdots & \cdots & \cdots & \cdots & \cdots & \cdots & \cdots & \cdots & \vdots & \\ & \vdots & 1 & 0 & \cdots & \cdots & 0 & 1 & -1 & \vdots & \\ & 0 & \cdots & \cdots & \cdots & \cdots & \cdots & \cdots & 1 & -1 & \\ &&&&&&&&&& \ddots \end{bmatrix}\begin{bmatrix} \dot{I}_1 \\ \dot{I}_2 \\ \vdots \\ \dot{I}_9 \\ \vdots \\ \dot{I}_{12} \\ \dot{I}_{13} \\ \vdots \\ \dot{I}_{20} \end{bmatrix}$$

$$=\begin{bmatrix} \dot{I}_1-\dot{I}_2 \\ \vdots \\ \dot{I}_{11}-\dot{I}_{12} \\ \vdots \\ \dot{I}_{12}-\dot{I}_{16}-\dot{I}_{17} \\ \dot{I}_{17}-\dot{I}_{18} \\ \dot{I}_{18}-\dot{I}_{20} \end{bmatrix}=\begin{bmatrix} \sum\dot{I}_{\varphi 1} \\ \sum\dot{I}_{\varphi 2} \\ \vdots \\ \sum\dot{I}_{\varphi 9} \\ \vdots \\ \sum\dot{I}_{\varphi 12} \\ \sum\dot{I}_{\varphi 13} \\ \sum\dot{I}_{\varphi 14} \end{bmatrix}=\begin{bmatrix} \dot{P}_{\varphi 1} \\ \dot{P}_{\varphi 2} \\ \vdots \\ \dot{P}_{\varphi 9} \\ \vdots \\ \dot{P}_{\varphi 12} \\ \dot{P}_{\varphi 13} \\ \dot{P}_{\varphi 14} \end{bmatrix}=\begin{bmatrix} \vdots \\ 0.141 \\ \vdots \\ 9.854 \\ 0.066 \\ 0.132 \end{bmatrix}$$

The setting current I_{set1} is calculated according to Eq. (4):

$$\begin{aligned} I_{set1} &= K_k K_{LH} K_f I_{d.\max} \\ &= 1.3\times 0.1\times 1.5\times 530.48 \\ &= 103.4436A \end{aligned} \tag{6}$$

Where K_k is the reliability coefficient of 1.3; K_{LH} is the current transformer ratio error of 0.1; K_f is the non-periodic component coefficient of 1.5; $I_{d.max}$ is the maximum short-circuit current flowing through the protection when the external short-circuit of bus differential protection occurs.

Based on the condition of short circuit in the area of unilateral power supply line, the protection sensitivity is checked:

$$K_l = \frac{I_{d.\min}}{I_{set1}} = \frac{302.85}{103.44} = 2.92 \geq 2 \tag{7}$$

Among them, $I_{d.min}$ represents the minimum short-circuit current flowing through the protection during an external fault in the bus differential protection zone. This parameter is introduced to ensure the reliability of the algorithm.

4.2 Single fault at different system locations

Assume that the AB two-phase short-circuit fault occurs at 9 lines of the node, that is, when F1 is at 0.5s. Similarly, the fault location matrix P_1 is generated according to the method described in the previous section:

$$P_1 = \begin{bmatrix} \vdots \\ \dot{P}_{A9} \\ \vdots \\ \dot{P}_{A12} \\ \dot{P}_{A13} \\ \vdots \end{bmatrix} = \begin{bmatrix} \vdots \\ 409.28 \\ \vdots \\ 3.862 \\ 2.932 \\ \vdots \end{bmatrix} \quad P_2 = \begin{bmatrix} \vdots \\ 0.196 \\ \vdots \\ 342.75 \\ 2.11 \\ \vdots \end{bmatrix} \quad P_3 = \begin{bmatrix} \vdots \\ 7.69 \\ \vdots \\ 6.381 \\ 343.81 \\ \vdots \end{bmatrix}$$

From the fault location matrix, the current of the remaining nodes is less than the set value I_{set1}, which can be ignored. At this time, the differential current of the line where the node 9 is located is greater than the threshold value, which meets the criteria, so it can be judged that the fault is located at the equivalent node 9. Fig.2 (a) is the effective value waveform of differential current at node 9, node 12 and node 13 when F1 fault occurs.

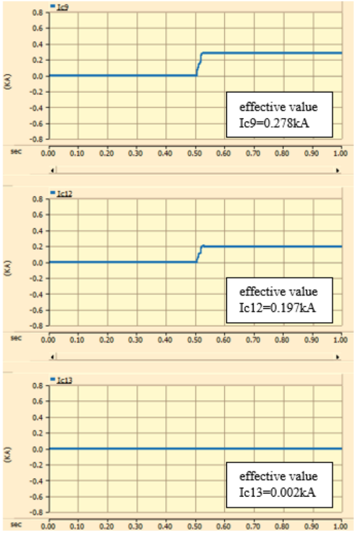

Fig. 3 The effective value waveform of differential current of each node under multiple faults

Assuming that AB two-phase short-circuit faults occur at node 12, namely F2, and node 13, namely F3, respectively, the fault location matrices P_2 and P_3 can be obtained.

From P_2, it can be judged that the F2 fault is located at 12 bus nodes. It can be obtained from P_3, so it can be judged that the F3 fault is located at 13 bus nodes. When F2 fault and F3 fault occur, the effective value waveforms of differential current at node 9, node 12 and node 13 of fault partition are shown in figure 2 (b) and (c) respectively, and the judgment is also accurate.

4.3 Multiple faults at different system locations.

It is assumed that two-phase short-circuit faults occur simultaneously at line node 9 and bus node 12, namely F1 and F2. At this time, the fault location matrix P_{12} is:

$$P_{12} = \begin{bmatrix} \vdots \\ 277.55 \\ \vdots \\ 196.61 \\ 1.918 \\ \vdots \end{bmatrix}$$

It can be observed from the row vector P_{12} that the values satisfy the predefined fault criterion, indicating the presence of faults at both Node 9 and Node 12. As illustrated in Figure 3, the RMS waveform of the differential currents across all nodes under multiple fault conditions further confirms the accuracy of the fault identification.

5. ADAPTABILITY ANALYSIS

Based on the differential protection principle, this scheme features a simple structure and reliable operation. It can be directly implemented using existing line measurement equipment, resulting in low modification costs, ease of implementation, and strong practical value for engineering applications. Simulation results verify that the algorithm maintains fault location accuracy under dynamic distributed generation output conditions, demonstrating strong adaptability in practical active distribution network operations.

It should be noted that line differential protection relies on comparing currents at both ends to detect faults. However, with the large-scale integration of distributed energy resources, distribution networks are expanding in coverage and line lengths are increasing. This increases the differential current, which may cause protection maloperation during normal operation, complicates fault setting, reduces operational reliability, and compromises power supply safety.

In the proposed scheme, losses due to long lines also necessitate higher fault setting values. During ground short-circuit faults, this may result in protection maloperation, requiring more careful configuration of setting value margins to ensure reliability. Further optimization of the setting values is required under high-impedance ground fault conditions to enhance the algorithm's practical robustness.

6. CONCLUSIONS

1) This paper introduces a matrix and current differential fusion-based method for fault location in distribution networks. It constructs a fault feature matrix by combining dynamic current and node differential matrices, enabling high-accuracy fault section identification in systems with distributed power sources.

2) The algorithm integrates with communication-based synchronous data acquisition systems, offering simplicity, low memory use, fast computation, and high accuracy. It provides a practical solution for active distribution networks with high renewable energy penetration.

3) Further research is needed to improve the method for future applications, including widespread renewable integration and AC/DC hybrid distribution networks.

FUNDING

This work is supported by National Natural Science Foundation of China (Grant No. U23B6007, Fundamental Theory and Methods for Form Evolution and High Efficient Safe Operation of New Power Distribution Systems)

REFERENCE

[1] Zhan, H., Liu, K., Sheng, W., et al. Review and Prospects of Fault Diagnosis and Location Methods for Active Distribution Networks. *High Voltage Engineering* 2023;49(2), 660–671.

[2] Luo, G., Zhao, Y., Wu, M., et al. An Improved Adaptive Current Protection Method for Distribution Networks with High Penetration of Renewable Energy Integration. *Distribution & Utilization* 2024;41(9), 12–23.

[3] Wang, B., & Chen, H. A Review of Improved Protection Schemes for Distribution Networks with Distributed Generation. *Power System Protection and Control* 2017;45(12), 146–154.

[4] Xie, L., Li, Y., Luo, L., et al. A Fault Location Method for Distribution Networks Based on Distance Matrix and Branch Coefficient. *Proceedings of the CSEE* 2020;40(7), 2180–2191+2397.

[5] Qi, Z., Ling, S., Liu, W., et al. Online Identification of Fault Nodes in Distribution Networks Based on High-Frequency Test Signal Injection. *Power System Protection and Control* 2020;48(4), 110–117.

[6] Lin, H., Wang, H., Zhang, K., et al. Research on Fault Location in Distribution Networks Based on Improved Two-Terminal Traveling Wave Method. *Electrotechnical Applications* 2023;(5), 88–90.

[7] Dai, Z., & Wang, X. A Fault Location Algorithm for Active Distribution Networks Based on Improved Impedance Method. *Power System Technology* 2017;41(6), 2027–2034.

[8] Xu, B., Yin, X., Zhang, Z., et al. Fault Location in Distribution Networks Based on a Combination of Matrix Algorithm and Optimization Algorithm. *Automation of Electric Power Systems* 2019;43(5), 152–158.

[9] Wang, X., Yue, Y., Guo, L., et al. A Fault Line Selection Method for Distribution Networks Based on Injected Current Distribution Characteristics. *Electric Power* 2024;57(10), 78–89.

[10] Lin, H., Wang, H., Zhang, K., et al. Research on Fault Location in Distribution Networks Based on Improved Two-Terminal Traveling Wave Method. *Electrotechnical Applications* 2023;(5), 88–90.

[11] Yang, C., Guo, W., Xiong, Y., et al. Fault Location Method for Under-Voltage Cross-Level Trip of Distribution Transformers Based on Improved Impedance Method. *Electrical Automation* 2023;45(3), 11–14.

[12] Zong, J., Liang, W., et al. A Protection Adaptability Evaluation Method for Distribution Networks with Distributed Generation Integration. *Journal of Electrical Engineering* 2025;1–11.

[13] Xu, S., Ouyang, J., Chen, Y., et al. A Single-Phase Grounding Fault Location Method for Active Distribution Networks Based on Model Identification. *Power System Protection and Control* 2024;52(5), 51–60.

[14] Zhang, P., Chen, Y., Wang, G., et al. Decision-Making for Distribution Network Fault Recovery Based on Graph Reinforcement Learning. *Automation of Electric Power Systems* 2024;48(2), 151–158.

[15] Wu, Y., Ma, Y., Wang, H., et al. Design and Implementation of a High-Speed Data Bus for WAMS in Grid Dispatch. *Automation Application* 2024;65(6), 185–192.